Axial electric field component in a fast ionization wave in nanosecond pulsed nitrogen discharge at 20-100 mbar

Tat Loon Chng, Inna Orel, Svetlana Starikovskaia, I.V. Adamovich

Axial Electric Field Component in a Fast Ionization Wave in Nanosecond Pulsed Nitrogen Discharge at 20-100 mbar

T.L. Chng[1], I.S. Orel[1], S.M. Starikovskaia[1] and I.V. Adamovich[2]

[1] *Laboratory of Plasma Physics (CNRS, Ecole Polytechnique, Sorbonne Universities, University of Pierre and Marie Curie - Paris 6, University Paris-Sud), Ecole Polytechnique, route de Saclay, 91128 Palaiseau, France*

[2]*Nonequilibrium Thermodynamics Laboratories, Department of Mechanical and Aerospace Engineering, Ohio State University, Columbus, OH 43210, USA*

Abstract: The axial electric field component in a fast ionization wave in ns tube discharge in N_2 at 20-100 mbar is measured by ps second harmonic generation with the temporal and spatial resolution of 200 ps and 0.5 mm respectively. From absolute calibration by current shunts, the peak axial electric field, 8-11 kV/cm, shows a weak dependence on pressure, with the peak reduced electric field ≈2000 Td at 20 mbar. For the same voltage conditions, pressure reduction from 100 to 20 mbar steepens the wave front from 3.0 ns to 1.0 ns FWHM.

Keywords: second harmonic generation, nanosecond plasma, FIW

1. Introduction

Discharges generated by high peak voltage, ns duration pulses have been studied extensively over the last two decades. At moderate pressures, from several mbar to several tens of mbar, the nanosecond pulse discharge develops as a Fast Ionization Wave (FIW), kinetics of which are reviewed in great detail in [1,2]. One of the most challenging aspects of characterization of kinetic processes in these plasmas, which occur on ns or even sub-ns time scales, is accurate diagnostics of electric field, electron density and temperature, and species number densities. A widely used method of electric field measurements in FIW discharges is by a calibrated capacitive probe [3,4], with a temporal resolution up to ~ 1 ns but a relatively low spatial resolution, ~ 1 cm. More recently, development and use of electro-optic probes has resulted in high temporal resolution (~ 1 ns), high spatial resolution (~ 1 mm) field measurements in atmospheric pressure plasma jets [5]. However, the presence of the probe perturbs the plasma to some extent, especially at the conditions when surface charge accumulation may occur on the probe housing. Development of non-intrusive, high spatio-temporal resolution diagnostics is essential for quantitative understanding of kinetics of ionization in the wave, charge transport and species generation in the plasma behind the wave front, and wave propagation and attenuation. The objective of the present work is to measure the electric field in a FIW, ns pulse discharge in nitrogen using the recently developed fs/ps Electric Field Induced Second Harmonic (E-FISH) diagnostic [6,7]. The principal advantages of usage of fs/ps laser on ns discharge are (i) sub-ns time resolution limited primarily by the sampling rate of the detector and the oscilloscope and (ii) reduced influence of laser shot on plasma due to the laser pulse duration which is shorter compared to the time scale of the electron impact ionization in the wave front or of the laser breakdown development.

2. Experimental

Figure 1 shows a schematic of ps E-FISH diagnostic similar to the one used in Ref. [7] together with the discharge cell's scheme. The discharge is sustained in a quartz tube with the internal diameter of 20 mm, between two hollow truncated cone brass electrodes separated by the distance of 8.0 cm. Nitrogen is flown through the tube at the flow rate of 10 sccm and the pressure of 20-100 mbar. The discharge in the tube is generated using positive polarity high-voltage pulses, with peak voltage of 9.3 kV, pulse rise/fall time of 4 ns, and pulse duration (FWHM) of 30 ns, at a repetition rate of 10 Hz, produced by an FPG 12-1NM (FID GmbH) high voltage pulse generator. The incident, reflected, and transmitted voltage pulse shapes are monitored by calibrated, high bandwidth current shunts [8,9] placed before the high-voltage electrode and after the grounded electrode. The vertically polarized 1064 nm fundamental output beam of a ps laser (EKSPLA PL2241, pulse 30 ps, pulse energy 6 mJ) is rotated to horizontal using a half-wave plate, and is directed across the quartz discharge tube halfway between the high-voltage and grounded electrodes, near its horizontal plane of symmetry. The beam is focused in the center of the tube by a 20 cm focal distance lens. A long pass filter, placed immediately after the focusing lens, is used to block the stray second harmonic signal generated in these components of the optical system. After exiting the discharge tube, the laser beam is collimated by a second 20 cm focal distance lens,

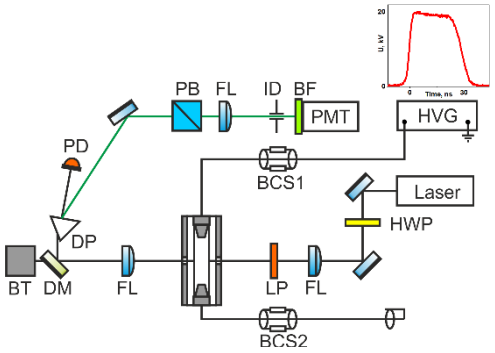

Figure 1. Schematic of the experimental apparatus and ps second harmonic generation diagnostic. BT: beam trap; DM: dichroic mirror (532 nm reflecting, 1064 nm transmitting); DP: dispersive prism; PD: photodiode; FL: plano-convex lens; PB: 532 nm polarizer; ID: iris diaphragm; BF: 532 nm bandpass filter; PMT: photomultiplier tube; LP: long pass filter; HWP: 1064 nm half-wave plate; HVG: high voltage generator; BCS1, BCS2: back current shunts before the high-voltage electrode and after the grounded electrode, respectively. The inset shows the voltage waveform on the high-voltage electrode, top view of the discharge tube is shown.

and the second harmonic signal is separated from the fundamental beam using a dichroic mirror and a dispersive prism. The intensity of the residual 1064 nm is monitored by a photodiode (PD) (Thorlabs DET10A, rise time 1 ns). The 532 nm second harmonic beam passes through a polarizer to isolate the horizontally polarized signal proportional to the square of the axial electric field in the discharge, and is focused into the IR H7422-50P Hamamatsu photomultiplier module (PMT) with a rise time of 1 ns. The PD and PMT signals are monitored by a digital oscilloscope (LeCroy WaveRunner 64Xi-A) with a 5 GHz sampling rate and 600 MHz bandwidth. The time-resolved plasma emission detected by the PMT during the discharge pulse (emission background) is measured with the laser turned off, and subtracted from the PMT signal measured with the laser on for the case of 20 mbar where the emission was seen to be important.

Single shot broadband plasma emission images of a ns pulse discharge in nitrogen at 20-100 mbar were taken using a Princeton Instruments PI-MAX 4 camera at consequent times to calculate the velocity of FIW front's propagation with the relative uncertainty of 5%. The sequence of shots illustrate clearly that the emission intensity is significantly lower when closer to the axis of symmetry meaning that the FIW is propagating predominantly near the walls of the discharge tube. The effect is more pronounced at higher pressures. Kinetic modelling predictions [4] reveal that this occurs due to the higher electric field near the wall, caused by the jump in permittivity, and due to the secondary photo-electron emission from the wall irradiated by the UV photons from the plasma.

During the data post-processing, the PD and PMT waveforms of every laser shot are placed into "time bins" 0.2 ns long (based on their timing relative to the transmitted current), integrated over time, and averaged, as was done in our previous work [10]. PMT signals indistinguishable from surrounding electro-magnetic noise were rejected and for a typical data set of 40,000 shots per pressure bin filling varies from ~20 to ~250 shots per bin. Statistical uncertainty is calculated as standard deviation using the Student's t-distribution for each bin and shown at Figures of the present paper in form of error bars. The laser output pulse energy, stability of which is critical for the accuracy of the electric field inference from the second harmonic signal, is monitored by the PD and its variation does not exceed a few percent. A separate data set is taken with a neutral density filter placed in front of the PMT, to verify that the PMT is operating in a linear regime.

3. Results and Discussion

The electric field calibration by a Laplacian field sustained between two parallel plate electrodes placed in the discharge tube 4 mm apart indicate that over the pressure range of 20-100 mbar, most of the second harmonic signal induced by the electric field in the discharge originates within the quartz wall of the discharge tube. For this reason, the absolute calibration of the electric field is obtained by comparing the second harmonic signal with the current shunt signals, after the FIW has reached the grounded electrode, i.e. at the conditions when the axial electric field distribution along the discharge gap is known to be uniform [11]. The detection limit of the present E-FISH measurements is approximately 0.5 kV/cm.

Figure 6(a-d) plots time-resolved, absolute axial electric field distributions in a FIW discharge in nitrogen at P=20-100 mbar, shown together with the current shunt signal used for absolute calibration at each time. The initial gradual rise of the signal corresponds to the Laplacian field generated ahead of the approaching ionization wave after it is initiated near the high-voltage electrode during the pulse voltage rise. The peak occurs when the ionization front arrives at the measurement location, and the electric field begins to decrease rapidly, due to the charge separation in the plasma generated in the wave. The electric field behind the wave is reduced considerably, but remains above the detection limit at all pressures tested, such that the electrons created in the wave front are transported toward the high-voltage electrode, generating the conduction current. The secondary rise of the electric field occurs after the wave front arrives at the grounded electrode (cathode), the secondary emission is generated from the cathode, and the discharge transitions into a quasi-steady-state regime. Finally, the electric field decays to near detection limit as the applied voltage is reduced to zero [3,4,8,9,11].

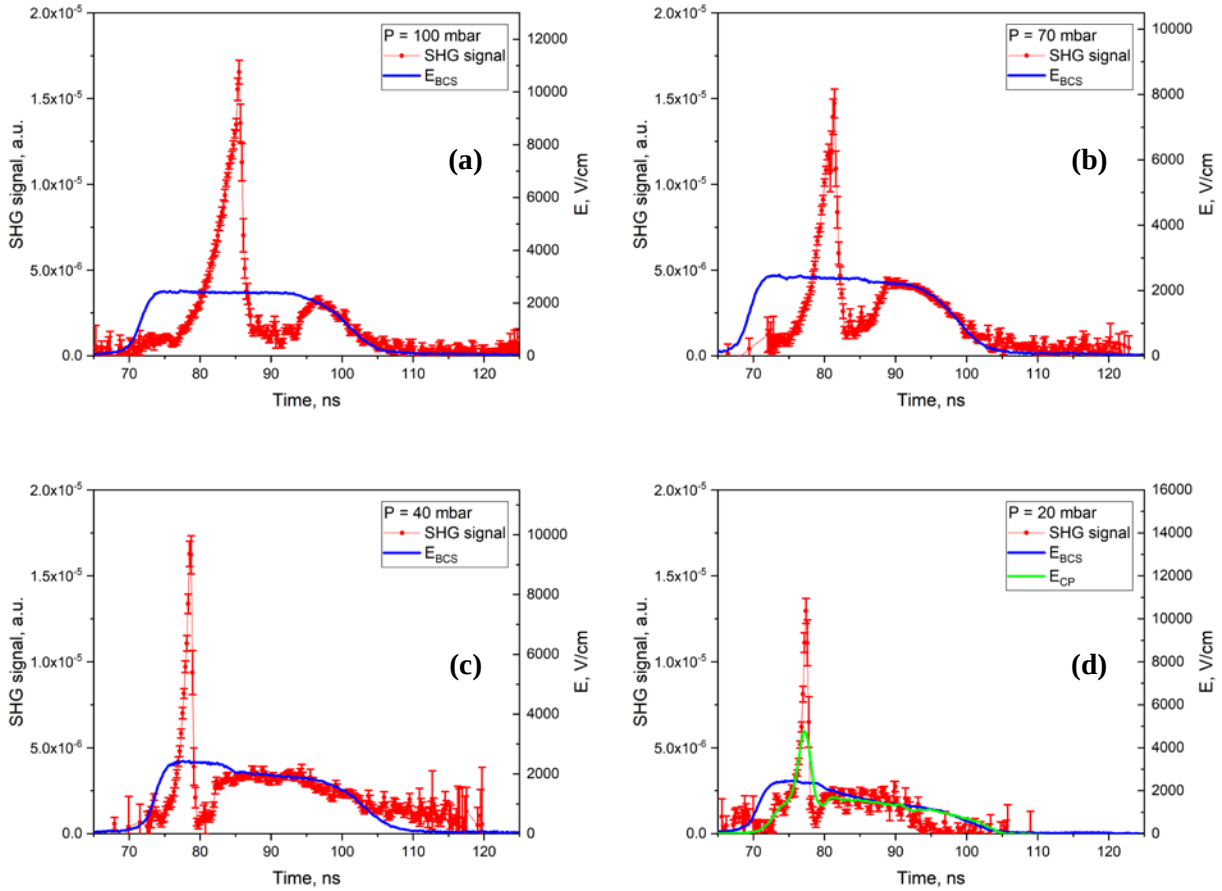

Figure 6. Electric field in a fast ionization wave discharge in nitrogen at P=20-100 mbar, plotted together with the current shunt signal used for absolute calibration (EBCS). Electric field inferred from the capacitive probe measurements (ECP) is also plotted at P=20 mbar.

It can be seen that the electric field waveform obtained by the E-FISH measurements matches the current shunt waveform after the moment when the wave reaches the grounded electrode (see Fig. 6(a-c), although at P=20 mbar the signal-to-noise ratio in the quasi-steady-state discharge becomes significantly lower (see Fig. 6(d)). At these low-pressure conditions, the emission from the quasi-steady-state discharge and the afterglow becomes much stronger, such that subtracting it from the PMT signal reduces the signal-to-noise. The effect of the plasma emission in the afterglow is also evident at P=40 mbar (see Fig. 6(c)), where it has not been subtracted from the signal. At P=20 mbar, additional comparison has been made with the electric field measured by a calibrated capacitive probe, described in detail in our previous work [2,11] (see Fig. 6(d)). The electric field peak in the ionization wave front, measured by the capacitive probe, is not fully resolved compared to the E-FISH data though it matches very well the current shunt waveform in the quasi-stead-state discharge. This behavior is expected, since the effective time resolution of the capacitive probe (~1.5-3.0 ns), limited by its spatial sensitivity, is up to an order of magnitude lower compared to that of the present E-FISH diagnostic (200 ps).

Comparison of the data taken at different pressures exhibits several dominant trends. First, in the entire pressure range, the peak electric field in the ionization wave exceeds the quasi-steady-state value established after the wave reaches the grounded electrode, by up to a factor of 4 to 5. Second, the peak value of the axial electric field in the wave front exhibits a fairly weak pressure dependence, E_{peak}=8-11 kV/cm (compare Figs. 6(a-d)). The highest reduced electric field, E/N≈2000 Td (assuming room temperature in the discharge), is produced at the lowest pressure of P=20 mbar, as expected (see Fig. 7). Third, reducing the pressure from 100 to 20 mbar, while keeping the discharge pulse voltage waveform the same, steepens the ionization wave front considerably, as illustrated in Fig. 7. At 100 mbar, the full width at half maximum of the transient electric field peak in the wave front is 3.0 ± 0.2 ns, while at 20 mbar it is reduced to 1.0 ± 0.2 ns, and remains fully resolved by the present diagnostic. This behavior is most likely due to the faster

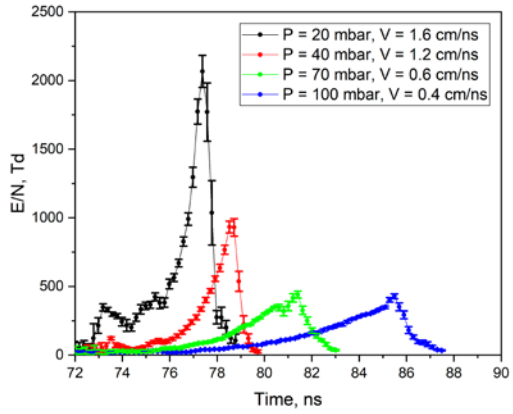

Figure 7. Reduced electric field in a fast ionization wave discharge in nitrogen at P=20-100 mbar, plotted on the same scale.

electron impact ionization at a significantly higher reduced electric field in the wave, as well as the more rapid electron transport behind the wave front, resulting in plasma self-shielding on a sub-ns time scale. Finally, the wave speed increases considerably as the pressure is reduced, from V = 0.4 cm/ns at 100 mbar to V = 1.6 cm/ns at 20 mbar. The wave speed values are indicated in the legend of Fig. 7.

4. Summary

In this work, non-intrusive, time-accurate, absolute measurements of the electric field in a FIW discharge sustained over a wide range of pressures are obtained for the first time. Since the present results are based on the detection of the electric field within the discharge tube wall, ps second harmonic generation using the present approach may be employed for electric field measurements at the conditions when the detection of the second harmonic signal generated directly in the plasma is challenging, i.e. (i) at low pressures, (ii) in small diameter capillary tubes, and (iii) in gases with very low nonlinear polarizability, such as helium. These results also show that the contribution of the discharge cell walls into the net electric-field induced second harmonic signal has to be identified and accounted for, e.g. using the electrostatic calibration over a wide range of pressures. Since the signal generated within the wall during the discharge is induced by the electric field, it cannot be easily subtracted from the net second harmonic signal, unlike the zero-field background. In principle, the temporal resolution of the present measurements is limited only by the laser pulse duration, in present work 30 ps, and may be improved further by using an oscilloscope with a higher sampling rate. In low and moderate pressure FIW discharges, this opens a possibility of detection and analysis of non-local electron kinetics effects in the presence of rapidly varying, high peak value reduced electric field. Finally, with additional calibration, the same approach can also be used to measure the radial component of the electric field in the ionization wave front, which has not been measured previously, and is known to control the wave propagation [1,2].

5. Acknowledgements

The work was partially supported by French National Research Agency, ANR (ASPEN Project), LabEx Plas@Par and the French–Russian international laboratory LIA KaPPA ‘Kinetics and Physics of Pulsed Plasmas and their Afterglow’. The experiments were conducted at the Centre Laser de l’Université Paris Sud (CLUPS/LUMAT FR 2764). The authors are thankful to Ali Mahjoub, Bruno Dufour and Pascal Pariset for technical assistance, and to Dr. Michel Broquier and Dr. Gilles Grégoire for helping setting up these experiments. The support of Prof. Adamovich by the Ecole Polytechnique Gaspard Monge Visiting Professor (GMVP) Program is gratefully acknowledged.

6. References

[1] L.M. Vasilyak, S.V. Kostyuchenko, N.N. Kudryavtsev, I.V. Filyugin, Physics-Uspekhi, 37, 247 (1994)

[2] S.M. Starikovskaia, N.B. Anikin, S.V. Pancheshnyi, D.V. Zatsepin and A.Yu. Starikovskii, Plasma Sources Science and Technology, 10, 344 (2001)

[3] N.B. Anikin, S.M. Starikovskaia, and A.Yu.Starikovskii, Journal of Physics D: Applied Physics, 35, 2785 (2002)

[4] K. Takashima, I.V. Adamovich, Z. Xiong, M.J. Kushner, S. Starikovskaia, U. Czarnetzki, and D. Luggenhölscher, Physics of Plasmas, 18, 083505 (2011)

[5] T. Darny, J.-M. Pouvesle, V. Puech, C. Douat, S. Dozias, and E. Robert, Plasma Sources Science and Technology, 26, 045008 (2017)

[6] A. Dogariu, B.M. Goldberg, S. O’Byrne, and R.B. Miles, Physical Review Applied, 7, 024024 (2017)

[7] B.M. Goldberg, T.L. Chng, A. Dogariu, and R.B. Miles, Applied Physics Letters, 112, 064102 (2018)

[8] N.B. Anikin, S.V. Pancheshnyi, S.M. Starikovskaia, and A.Yu.Starikovskii, Journal of Physics D: Applied Physics, 31, 826 (1998)

[9] N.B. Anikin, S.M. Starikovskaia, and A.Yu.Starikovskii, Plasma Physics Reports, 30, 1028 (2004)

[10] B.M. Goldberg, I. Shkurenkov, S. O’Byrne, I.V. Adamovich, and W.R. Lempert, Plasma Sources Science and Technology, 24, 035010 (2015)

[11] A.V. Klochko, S.M. Starikovskaia, Zh. Xiong, and M.J. Kushner, Journal of Physics D: Applied Physics, 47, 365202 (2014)